Experimental Liquidus in the PbO-ZnO-"Fe_2O_3"-($CaO + SiO_2$) System in Air, with $CaO/SiO_2 = 0.35$ and $PbO/(CaO + SiO_2) = 3.2$

EVGUENI JAK and PETER C. HAYES

Experimental studies on phase equilibria in the multicomponent system PbO-ZnO-CaO-SiO_2-FeO-Fe_2O_3 in air have been conducted to characterize the phase relations of a complex slag system used in lead and zinc smelting. The liquidus in the pseudoternary section ZnO-"Fe_2O_3"-(PbO + CaO + SiO_2) with a CaO/SiO_2 weight ratio of 0.35 and a $PbO/(CaO + SiO_2)$ weight ratio of 3.2 has been constructed to describe liquidus temperatures as a function of composition in the range of commercial operating conditions employed by the Lead Isasmelt smelting process. The section contains the primary phase fields of spinel (zinc ferrite, $Zn_xFe_{3-y}O_{4+z}$), zincite ($Zn_uFe_{1-u}O$), melilite ($Pb_vCa_{2-v}Zn_wFe_{1-w}Si_2O_7$), hematite ($Fe_2O_3$), magnetoplumbite ($PbFe_{10}O_{16}$), and wollastonite ($CaSiO_3$).

I. INTRODUCTION

THE first stage of the Lead Isasmelt process involves the oxidation smelting of lead sulfides in oxygen-enriched air to produce a lead-rich slag.[1,2] Sulfur is removed from the melt into the gas phase. The principal components of the resultant slag are PbO, ZnO, CaO, SiO_2, FeO, and Fe_2O_3.

Previous investigations of phase equilibria in lead and zinc blast-furnace slags have described phase relations in these systems by simplifying them to four components and have reported a series of pseudoternary sections at fixed concentrations of the fourth component. For instance, Manson and Segnit[3] constructed several sections of the CaO-ZnO-SiO_2 system with various alumina contents. Kato *et al.*[4] presented a section of CaO-Al_2O_3-SiO_2 with 50 wt pct FeO to describe a zinc blast-furnace slag. Lenz and Lee[5] reported a part of a section of FeO-CaO-SiO_2 at 12.5 wt pct ZnO. None of the previous systems contains PbO.

Preliminary experimental studies of phase equilibria for the zinc and lead blast-furnace sinters in air are reported by Lee,[6] Lee *et al.*,[7] and Nairn.[8] The materials in those studies contained lead oxide, adding an extra degree of complexity to the problem. It was reported that the primary phases in these slags are spinel (zinc ferrite, $Zn_xFe_{3-y}O_{4+z}$), zincite ($Zn_uFe_{1-u}O$), and melilite ($Pb_vCa_{2-v}Zn_wFe_{1-w}Si_2O_7$).

There has been no systematic study reported in the literature on the liquidus temperatures and primary phases formed in these lead-smelting slags. The principal reasons for this appear to be as follows. The high number of variables in such a six-component system indicates that a large number of experiments are required to fully characterize the system. There is also a significant problem in presenting results in a useful form. In addition, there are experimental difficulties associated with the high-temperature equilibration of these melts, for example, PbO and ZnO losses through vaporization and containment of aggressive slags.

EVGUENI JAK, Research Director, and PETER C. HAYES, Director, Associate Professor, are with PYROSEARCH, Pyrometallurgy Research Centre, School of Engineering, The University of Queensland, Brisbane, Queensland, 4072, Australia. Contact e-mail: E.Jak@minmet.uq.edu.au

Manuscript submitted April 1, 2002.

The aims of this article are to demonstrate a methodology that enables the systematic analysis of phase equilibria in this system to be undertaken, and to supply information on the liquidus temperatures of these slags in a form which is readily interpreted and which can be used in commercial lead pyrometallurgical operations.

This experimental study on the PbO-ZnO-"Fe_2O_3"-(CaO + SiO_2) system in air is part of a wider overall experimental program that combines experimental investigations with thermodynamic modeling to characterize phase relations and thermodynamic properties in the six-component system PbO-ZnO-SiO_2-CaO-FeO-Fe_2O_3 over a wide range of compositions important to zinc/lead industrial smelting processes. Studies of a number of subsystems within this overall research program have already been described in previous publications by the present authors.[9–28]

II. EXPERIMENTAL METHODOLOGY

A. *Selection of the Pseudoternary Section*

Pseudoternary sections are used to describe the phase equilibria in the multicomponent systems in the range of compositions of interest, so that the liquidus temperatures can be uniquely described as a function of composition and can be projected as isotherms on a two-dimensional equilateral triangular base. The appropriate choice of end members can result in the construction of joins that could be regarded as ternary systems. If all of the crystalline phases have compositions in the plane of the section, then these ternary sections can be interpreted in the same way as ternary-phase diagrams, *e.g.*, the lever rule can still be applied to determine the proportions of the phases present at any temperature. The crystallization path of any liquid, therefore, can be traced. If compounds are formed that do not contain the same stoichiometric ratios as end members, then this part of system does not obey the general rules of a ternary diagram.

Preliminary equilibration and quenching experiments have been performed to identify primary phases of the lead smelting slags, to assist in selection of the form of the pseudoternary sections. Examination of the microstructures

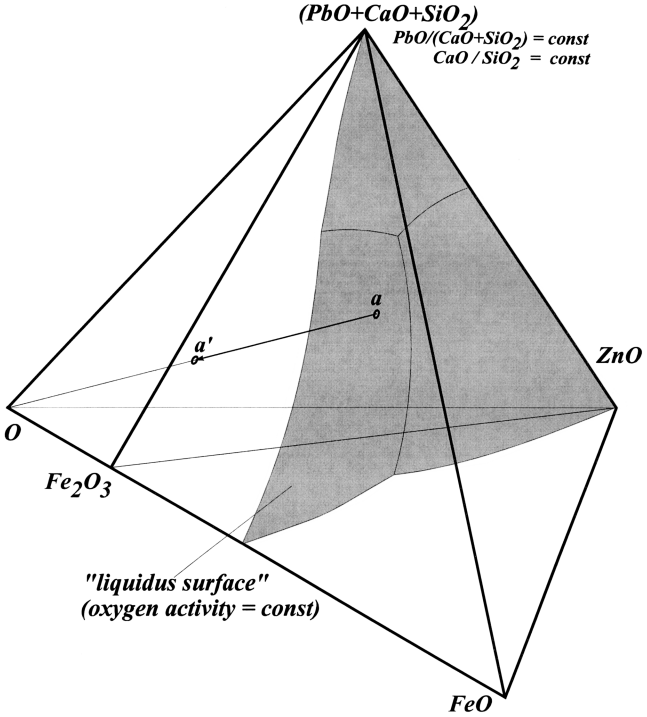

Fig. 1—Composition tetrahedron with the constant PbO/(CaO + SiO_2) and CaO/SiO_2 ratios.

of the preliminary experiments for the samples in the composition range of interest to lead smelting slags indicated that the initial crystallization followed the sequence: (1) the primary precipitation of zincite, spinel, or melilite, depending on the bulk mixture composition; (2) the "binary eutectic" crystallization of zincite + spinel, zincite + melilite, or spinel + melilite, depending on the mixture composition; and (3) the "ternary eutectic" crystallization reaction of zincite + spinel + melilite. From the information obtained in these preliminary studies, it was decided to construct pseudoternary sections formed by zincite and iron oxide in two apexes and the sum of PbO, CaO, and SiO_2 in the third. The PbO, CaO, and SiO_2 proportions will be expressed as the PbO/(CaO + SiO_2) and CaO/SiO_2 ratios.

Selection of the compositional ratios in the apex (PbO + CaO + SiO_2) depends on the particular slag system of interest. The present article focuses on the pseudoternary section investigated for the Lead Isasmelt process with low-lead slags. The lime-to-silica ratio of particular interest to the Lead Isasmelt process is approximately 0.35.[13] The lead oxide content depends on the feed materials and on the lead concentrate grade and is an average of approximately 45 wt pct for the low-lead Isasmelt slags, which corresponds to the PbO/(CaO + SiO_2) weight ratio of 3.2.

B. *Analysis of Number of Degrees of Freedom*

The ratio of Fe_2O_3 to FeO depends on both temperature and oxygen activity, so the gas phase has to be included in any analysis of the number of degrees of freedom. Assuming that air consists of only oxygen and nitrogen, the number of C elements in the present system Pb-Zn-Ca-Si-Fe-O-N is equal to seven. For a liquid in equilibrium with one solid phase and the gas phase, the number of degrees of freedom

Table I. Mixture Compositions Used for Experiments on the Section CaO/SiO_2 = 0.35, PbO/(CaO + SiO_2) = 3.2

Mixture Number	Composition of Mixture (Wt Pct)				
	Fe_2O_3	ZnO	PbO	CaO	SiO_2
50	40.0	0.0	45.7	3.7	10.6
51	23.2	11.8	49.5	4.0	11.5
52	18.0	20.0	47.2	3.8	10.9
53	10.0	21.0	52.6	4.3	12.2
54	0.0	22.0	59.4	4.8	13.8
55	3.0	25.0	54.9	4.4	12.7
56	20.0	4.0	57.9	4.7	13.4
57	23.3	5.0	54.6	4.4	12.6
58	27.5	4.7	51.7	4.2	12.0
59	28.5	1.5	53.3	4.3	12.3
60	18.0	6.0	57.9	4.7	13.4
61	14.3	11.5	56.5	4.6	13.1
62	12.8	14.8	55.2	4.5	12.8
63	15.9	8.1	57.9	4.7	13.4
64	2.0	16.0	62.5	5.1	14.5
65	2.0	13.5	64.4	5.2	14.9
66	2.0	11.0	66.3	5.4	15.3
67	2.0	7.5	69.0	5.6	16.0
68	6.0	15.0	60.2	4.9	13.9
69	6.0	12.0	62.5	5.1	14.5
691	6.0	9.2	64.6	5.2	15.0
692	6.5	6.0	66.7	5.4	15.4
693	4.0	4.0	70.1	5.7	16.2
694	9.0	2.0	67.8	5.5	15.7
695	18.0	1.5	61.3	5.0	14.2
696	27.8	3.5	52.3	4.2	12.1
697	28.2	2.5	52.8	4.3	12.2
681	1.5	1.5	73.9	6.0	17.1
682	3.5	1.0	72.8	5.9	16.8
683	1.0	3.5	72.8	5.9	16.8
684	3.0	3.0	71.6	5.8	16.6
685	1.0	5.0	71.6	5.8	16.6
686	6.8	1.0	70.2	5.7	16.3
687	12.0	1.0	66.3	5.4	15.3
688	10.0	3.0	66.3	5.4	15.3
689	14.8	1.0	64.2	5.2	14.9

is $F = C + 2 - P = 7 + 2 - 3 = 6$. Since the CaO/$SiO_2$ and PbO/(CaO + SiO_2) ratios of the liquid phase were fixed and experiments were carried out in air (total pressure and oxygen potential were fixed), then four degrees of freedom were expended and only two remain. This means that the compositions of all liquids, which have certain CaO/SiO_2 and PbO/(CaO + SiO_2) ratios, in equilibrium with one solid at a fixed oxygen activity lie on a two-dimensional curved surface which will be referred to as the "liquidus surface." This is illustrated schematically in Figure 1. The liquidus surface is located within the composition tetrahedron ZnO-(PbO + CaO + SiO_2)-FeO-Fe_2O_3. Each particular point on the liquidus surface determines the primary phase, liquidus temperature, and FeO/Fe_2O_3 ratio. Similarly, the compositions of the liquids in equilibrium with two solids and the gas phase will form a line which will be called the "boundary line." It should be remembered that the liquidus surface defined previously is a two-dimensional section through five-dimensional space, where CaO/SiO_2, PbO/(CaO + SiO_2), and the oxygen activity can also be independently varied within certain limits. No nitrogen-containing condensed phases were observed to be stable in the range of conditions investigated.

Table II. Experimental Data on the Section $CaO/SiO_2 = 0.35$ and $PbO/(CaO + SiO_2) = 3.2$

Experiment Number	Temperature (°C)	Mixture Number	Phases in Equilibrium	Phase Name	Phase Composition (Wt Pct)					C/S Wt	P/CS Wt
					Fe_2O_3	ZnO	PbO	CaO	SiO_2		
				Equilibria [Liquid + Air]							
371	1023	689	L.	L.	14.8	1.1	64.1	5.2	14.8	0.35	3.20
370	1023	687	L.	L.	11.9	1.0	66.2	5.3	15.6	0.34	3.17
369	1053	688	L.	L.	10.1	3.0	66.1	5.3	15.5	0.34	3.18
368	1053	686	L.	L.	6.9	1.0	69.9	5.7	16.5	0.35	3.15
374	1083	681	L.	L.	1.5	1.7	73.1	6.0	17.7	0.34	3.08
366	1088	681	L.	L.	1.6	1.6	73.3	6.0	17.5	0.34	3.12
364	1088	682	L.	L.	3.7	1.0	72.2	6.0	17.1	0.35	3.13
378	1093	683	L.	L.	1.0	3.6	72.3	5.9	17.2	0.34	3.13
373	1103	683	L.	L.	1.1	3.5	72.4	5.9	17.1	0.35	3.15
372	1133	685	L.	L.	1.0	5.2	71.0	5.8	17.0	0.34	3.11
342	1033	694	L.	L.	9.3	2.1	67.5	5.5	15.6	0.35	3.20
359	1033	689	L.	L.	15.0	1.0	64.2	5.1	14.7	0.35	3.24
322	1073	694	L.	L.	8.9	2.1	67.7	5.4	15.9	0.34	3.18
356	1073	684	L.	L.	3.1	3.2	71.2	5.9	16.6	0.36	3.16
316	1073	694	L.	L.	8.9	1.9	68.1	5.4	15.7	0.34	3.23
310	1093	695	L.	L.	17.9	1.5	61.3	5.0	14.3	0.35	3.18
352	1093	681	L.	L.	1.5	1.7	73.5	6.0	17.3	0.35	3.15
341	1103	693	L.	L.	4.0	4.2	70.0	5.8	16.0	0.36	3.21
340	1123	692	L.	L.	6.6	6.2	66.6	5.3	15.3	0.35	3.23
330	1143	68	L.	L.	6.3	15.5	59.4	4.8	14.0	0.34	3.16
318	1153	68	L.	L.	5.8	15.3	60.0	4.9	14.0	0.35	3.17
338	1153	691	L.	L.	6.3	9.7	63.6	5.3	15.1	0.35	3.12
344	1153	69	L.	L.	6.1	12.6	61.1	5.2	15.0	0.35	3.02
346	1153	67	L.	L.	2.0	7.8	68.5	5.6	16.1	0.35	3.16
329	1163	69	L.	L.	6.0	12.6	61.4	5.1	14.9	0.34	3.07
337	1163	64	L.	L.	2.2	16.6	61.7	5.1	14.4	0.35	3.16
343	1163	65	L.	L.	2.0	13.9	63.7	5.3	15.1	0.35	3.12
328	1173	65	L.	L.	2.0	14.4	62.8	5.4	15.4	0.35	3.02
336	1173	66	L.	L.	2.2	11.8	64.7	5.4	15.9	0.34	3.04
317	1183	64	L.	L.	1.9	16.6	61.7	5.1	14.7	0.35	3.12
249	1293	56	L.	L.	20.2	4.2	57.2	4.7	13.7	0.34	3.11
246	1293	53	L.	L.	10.5	22.4	49.5	4.5	13.1	0.34	2.81
				Equilibria [Liquid + Spinel + Air]							
305	1053	60	L.Sp.	L.	12.6	3.4	64.1	5.1	14.8	0.34	3.22
				Sp.	68.3	31.4	0.1	0.1	0.1		
274	1093	57	L.Sp.	L.	17.6	2.3	61.1	4.9	14.1	0.35	3.22
				Sp.	71.0	28.8	0.1	0.1	0.0		
239	1093	56	L.Sp.	L.	17.1	2.4	61.5	4.9	14.1	0.35	3.24
				Sp.	70.7	29.0	0.2	0.1	0.0		
277	1093	60	L.Sp.	L.	13.7	3.9	62.7	5.0	14.7	0.34	3.18
				Sp.	68.7	31.1	0.1	0.0	0.1		
295	1093	63	L.Sp.	L.	11.4	6.2	63.0	5.0	14.4	0.35	3.25
				Sp.	67.9	31.4	0.5	0.1	0.1		
294	1113	63	L.Sp.	L.	11.6	6.2	62.5	5.1	14.6	0.35	3.17
				Sp.	68.2	31.4	0.4	0.0	0.0		
302	1133	61	L.Sp.	L.	9.9	9.9	61.0	4.9	14.3	0.34	3.18
				Sp.	67.2	32.7	0.1	0.0	0.0		
278	1143	61	L.Sp.	L.	10.0	10.1	60.4	5.0	14.5	0.34	3.10
				Sp.	67.6	32.4	0.0	0.0	0.0		
279	1143	62	L.Sp.	L.	8.2	13.6	58.8	4.9	14.5	0.34	3.03
				Sp.	66.8	33.1	0.0	0.0	0.1		
293	1143	63	L.Sp.	L.	12.8	6.7	61.2	5.0	14.3	0.35	3.17
				Sp.	67.9	31.5	0.5	0.0	0.1		
301	1163	58	L.Sp.	L.	22.2	2.3	57.6	4.5	13.4	0.34	3.22
				Sp.	74.7	24.9	0.3	0.1	0.0		
268	1193	57	L.Sp.	L.	20.3	3.6	57.7	4.7	13.7	0.34	3.14
				Sp.	72.1	27.6	0.2	0.1	0.0		
242	1193	56	L.Sp.	L.	20.3	4.2	57.4	4.7	13.4	0.35	3.17
				Sp.	72.1	27.6	0.2	0.1	0.0		
272	1193	61	L.Sp.	L.	11.2	10.5	59.1	4.9	14.3	0.34	3.08
				Sp.	67.7	32.1	0.1	0.0	0.1		
292	1193	63	L.Sp.	L.	14.3	7.4	59.5	4.8	14.0	0.34	3.16
				Sp.	68.5	31.1	0.3	0.0	0.1		

Table II. Experimental Data on the Section $CaO/SiO_2 = 0.35$ and $PbO/(CaO + SiO_2) = 3.2$—Continued

Experiment Number	Temperature (°C)	Mixture Number	Phases in Equilibrium	Phase Name	Phase Composition (Wt Pct)					C/S Wt	P/CS Wt
					Fe_2O_3	ZnO	PbO	CaO	SiO_2		
				Equilibria [Liquid + Spinel + Air]-Continued							
271	1193	60	L.Sp.	L.	17.0	5.7	58.4	4.8	14.1	0.34	3.09
				Sp.	70.1	29.8	0.1	0.0	0.0		
226	1193	52	L.Sp.	L.	9.4	18.4	54.8	4.7	12.7	0.37	3.15
				Sp.	67.0	32.8	0.1	0.0	0.1		
269	1193	58	L.Sp.	L.	23.1	2.7	55.9	4.7	13.6	0.35	3.05
				Sp.	74.7	25.0	0.2	0.1	0.0		
273	1193	62	L.Sp.	L.	10.1	14.4	56.8	4.7	14.0	0.34	3.04
				Sp.	67.3	32.7	0.0	0.0	0.0		
332	1193	696	L.Sp.	L.	24.7	2.4	55.4	4.5	13.0	0.35	3.17
				Sp.	76.6	23.0	0.3	0.1	0.0		
361	1243	696	L.Sp.	L.	27.0	3.0	53.1	4.4	12.5	0.35	3.14
				Sp.	77.3	22.5	0.1	0.1	0.0		
245	1293	52	L.Sp.	L.	14.4	19.8	49.3	4.2	12.3	0.34	2.99
				Sp.	67.7	32.1	0.1	0.0	0.1		
244	1293	51	L.Sp.	L.	18.2	10.1	53.9	4.6	13.2	0.35	3.03
				Sp.	70.0	29.9	0.1	0.0	0.0		
				Equilibria [Liquid + Magneto-Plumbite + Air]							
376	1013	689	L.P.	L.	14.5	1.1	64.3	5.2	14.9	0.35	3.20
				P.	75.4	0.8	22.9	0.2	0.7		
280	1043	59	L.P.	L.	15.2	1.5	62.4	5.3	15.6	0.34	2.99
				P.	78.1	1.0	20.7	0.1	0.1		
321	1073	695	L.P.	L.	17.0	1.5	62.0	5.0	14.5	0.34	3.18
				P.	78.1	1.1	20.7	0.0	0.1		
331	1083	695	L.P.	L.	17.7	1.6	61.5	4.9	14.3	0.34	3.20
				P.	78.9	0.8	20.0	0.1	0.2		
				Equilibria [Liquid + Melilite + Air]							
358	1043	688	L.Mel.	L.	10.0	3.0	66.4	5.3	15.3	0.35	3.22
				Mel.	1.4	21.4	9.2	31.6	36.4		
367	1053	684	L.Mel.	L.	3.0	2.6	72.6	5.4	16.4	0.33	3.33
				Mel.	0.6	20.9	13.6	29.7	35.2		
375	1063	684	L.Mel.	L.	3.1	3.0	71.8	5.4	16.7	0.32	3.25
				Mel.	0.5	22.1	9.7	31.1	36.6		
315	1073	693	L.Mel.	L.	4.3	3.5	71.5	5.0	15.7	0.32	3.45
				Mel.	0.6	21.7	9.4	31.4	36.9		
314	1073	692	L.Mel.	L.	6.9	4.9	70.6	3.7	13.9	0.27	4.01
				Mel.	0.7	21.7	12.1	30.0	35.5		
313	1073	67	L.Mel.	L.	2.2	6.4	74.1	3.2	14.1	0.23	4.28
				Mel.	0.2	22.4	12.1	29.8	35.5		
355	1083	683	L.Mel.	L.	0.9	3.5	72.9	5.7	17.0	0.34	3.21
				Mel.	0.1	22.0	9.9	31.6	36.4		
365	1088	683	L.Mel.	L.	1.0	3.6	72.4	6.0	17.0	0.35	3.15
				Mel.	0.4	21.6	10.6	31.1	36.3		
353	1093	685	L.Mel.	L.	1.1	4.5	73.4	5.0	16.0	0.31	3.50
				Mel.	0.1	22.4	10.3	31.1	36.1		
327	1093	693	L.Mel.	L.	4.0	4.0	70.1	5.6	16.3	0.34	3.20
				Mel.	0.5	21.9	9.1	31.6	36.9		
325	1103	67	L.Mel.	L.	2.1	6.7	72.3	4.1	14.8	0.28	3.83
				Mel.	0.2	22.1	11.4	30.6	35.7		
326	1103	692	L.Mel.	L.	6.5	5.7	68.0	4.8	15.0	0.32	3.43
				Mel.	0.7	22.2	9.5	31.3	36.3		
311	1113	66	L.Mel.	L.	2.1	10.5	69.5	3.6	14.3	0.25	3.88
				Mel.	0.2	22.8	10.2	30.8	36.0		
363	1113	685	L.Mel.	L.	1.0	5.0	71.9	5.5	16.6	0.33	3.25
				Mel.	0.1	22.2	10.2	31.1	36.4		
348	1113	692	L.Mel.	L.	6.6	5.8	67.4	5.1	15.1	0.34	3.34
				Mel.	0.8	21.5	10.3	31.2	36.2		
308	1123	65	L.Mel.	L.	2.0	13.6	66.5	3.8	14.1	0.27	3.72
				Mel.	0.1	23.1	9.6	31.2	36.0		
377	1123	685	L.Mel.	L.	1.0	5.4	70.8	5.8	17.0	0.34	3.11
				Mel.	0.1	22.1	9.5	31.4	36.9		
309	1123	69	L.Mel.	L.	6.3	11.9	63.5	4.4	13.9	0.32	3.47
				Mel.	0.8	21.9	11.7	30.0	35.6		

Table II. Experimental Data on the Section $CaO/SiO_2 = 0.35$ and $PbO/(CaO + SiO_2) = 3.2$—Continued

Experiment Number	Temperature (°C)	Mixture Number	Phases in Equilibrium	Phase Name	Phase Composition (Wt Pct)					C/S Wt	P/CS Wt
					Fe_2O_3	ZnO	PbO	CaO	SiO_2		
				Equilibria [Liquid + Melilite + Air]-Continued							
307	1133	68	L.Mel.	L.	6.2	14.7	62.2	3.8	13.1	0.29	3.68
				Mel.	0.3	23.0	7.7	32.1	36.9		
324	1143	691	L.Mel.	L.	6.1	9.4	63.8	5.3	15.4	0.34	3.08
				Mel.	0.4	22.7	8.6	31.8	36.5		
347	1143	64	L.Mel.	L.	2.0	16.6	62.9	4.4	14.1	0.31	3.40
				Mel.	0.1	23.1	8.4	32.0	36.4		
319	1143	65	L.Mel.	L.	2.3	13.5	65.7	4.2	14.3	0.29	3.55
				Mel.	0.1	23.1	8.5	31.8	36.5		
323	1143	66	L.Mel.	L.	2.0	11.1	67.7	4.4	14.8	0.30	3.53
				Mel.	0.2	22.5	8.9	31.5	36.9		
339	1143	67	L.Mel.	L.	2.1	7.5	69.1	5.4	15.9	0.34	3.24
				Mel.	0.1	22.8	8.8	31.8	36.5		
320	1143	69	L.Mel.	L.	6.0	12.5	62.2	5.0	14.3	0.35	3.22
				Mel.	0.4	22.7	8.1	32.1	36.7		
351	1153	65	L.Mel.	L.	2.1	14.0	64.0	4.9	15.0	0.33	3.22
				Mel.	0.1	23.2	8.2	31.6	36.9		
350	1153	64	L.Mel.	L.	2.1	16.6	62.2	4.7	14.4	0.33	3.26
				Mel.	0.2	22.8	9.9	30.8	36.3		
345	1163	66	L.Mel.	L.	2.2	11.6	65.1	5.4	15.7	0.34	3.09
				Mel.	0.2	23.1	8.4	31.9	36.4		
306	1173	64	L.Mel.	L.	2.5	20.6	52.6	6.1	18.2	0.34	2.16
				Mel.	0.2	23.0	9.2	31.3	36.3		
				Equilibria [Liquid + Wollastonite + Air]							
360	1013	687	L.CS.	L.	12.4	1.2	67.2	4.4	14.8	0.30	3.50
				CS.	0.1	0.0	2.5	47.0	50.4		
349	1023	694	L.CS.	L.	9.1	2.2	68.6	4.9	15.2	0.32	3.41
				CS.	0.3	0.2	1.9	47.3	50.3		
357	1043	686	L.CS.	L.	7.1	1.0	71.4	4.9	15.6	0.31	3.48
				CS.	0.1	0.0	2.2	47.2	50.5		
379	1073	681	L.CS.	L.	1.6	1.7	74.5	5.4	16.8	0.32	3.36
				CS.	0.0	0.0	2.6	46.8	50.6		
354	1083	682	L.CS.	L.	3.7	1.1	72.7	5.6	16.9	0.33	3.23
				CS.	0.0	0.0	2.2	47.2	50.6		
				Equilibria [Liquid + Hematite + Air]							
229	1093	50	L.Hem.	L.	17.8	0.0	64.0	5.0	13.2	0.38	3.52
				Hem.	100.0	0.0	0.0	0.0	0.0		
224	1193	50	L.Hem.	L.	22.8	0.0	60.0	4.6	12.6	0.37	3.49
				Hem.	99.9	0.0	0.1	0.0	0.0		
270	1193	59	L.Hem.	L.	25.4	1.7	55.4	4.5	13.0	0.35	3.17
				Hem.	99.9	0.1	0.0	0.0	0.0		
243	1293	50	L.Hem.	L.	33.2	0.0	50.6	4.1	12.1	0.34	3.12
				Hem.	99.9	0.0	0.1	0.0	0.0		
				Equilibria [Liquid + Zincite + Air]							
258	1153	55	L.Z.	L.	3.6	17.0	59.2	5.2	15.0	0.35	2.93
				Z.	0.2	99.8	0.0	0.0	0.0		
257	1163	54	L.Z.	L.	0.0	18.9	59.6	5.4	16.1	0.34	2.77
				Z.	0.0	99.8	0.1	0.0	0.1		
251	1163	55	L.Z.	L.	3.5	17.2	59.5	5.1	14.7	0.35	3.01
				Z.	0.1	99.9	0.0	0.0	0.0		
250	1173	54	L.Z.	L.	0.0	19.0	61.2	5.0	14.8	0.34	3.09
				Z.	0.0	100	0.0	0.0	0.0		
241	1193	55	L.Z.	L.	3.5	17.4	59.8	4.8	14.5	0.33	3.10
				Z.	0.2	99.8	0.0	0.0	0.0		
228	1193	54	L.Z.	L.	0.0	19.4	60.8	5.3	14.5	0.37	3.07
				Z.	0.0	99.9	0.1	0.0	0.0		
247	1293	54	L.Z.	L.	0.0	23.6	56.8	5.0	14.6	0.34	2.90
				Z.	0.0	99.9	0.1	0.0	0.0		
248	1293	55	L.Z.	L.	3.4	25.3	51.4	5.0	14.9	0.34	2.58
				Z.	0.2	99.7	0.1	0.0	0.0		

Table II. Experimental Data on the Section $CaO/SiO_2 = 0.35$ and $PbO/(CaO + SiO_2) = 3.2$—Continued

Experiment Number	Temperature (°C)	Mixture Number	Phases in Equilibrium	Phase Name	Phase Composition (Wt Pct)					C/S Wt	P/CS Wt
					Fe_2O_3	ZnO	PbO	CaO	SiO_2		
				Equilibria [Liquid + Spinel + Zincite + Air]							
260	1133	53	L.Sp.Z.	L.	7.4	17.1	57.6	4.6	13.3	0.35	3.22
				Sp.	65.2	33.9	0.1	0.0	0.8		
				Z.	0.9	99.0	0.0	0.1	0.0		
236	1143	53	L.Sp.Z.	L.	7.7	18.2	56.5	4.6	13.0	0.35	3.21
				Sp.	66.4	33.5	0.1	0.0	0.0		
				Z.	0.6	99.3	0.0	0.1	0.0		
227	1193	53	L.Sp.Z.	L.	8.5	20.8	53.5	4.6	12.6	0.37	3.11
				Sp.	66.7	33.2	0.0	0.0	0.1		
				Z.	0.6	99.0	0.3	0.0	0.1		
				Equilibria [Liquid + Spinel + Magneto-Plumbite + Air]							
256	993	56	L.Sp.P.	L.	12.7	2.0	64.9	5.2	15.2	0.34	3.18
				Sp.	68.6	30.7	0.5	0.1	0.1		
				P.	75.4	2.1	22.1	0.1	0.3		
263	1003	56	L.Sp.P.	L.	12.8	2.0	64.7	5.3	15.2	0.35	3.16
				Sp.	68.7	30.4	0.8	0.1	0.0		
				P.	74.9	2.1	22.4	0.2	0.4		
266	1043	56	L.Sp.P.	L.	15.2	1.6	63.3	5.1	14.8	0.34	3.18
				Sp.	69.0	28.8	1.9	0.1	0.2		
				P.	69.6	1.9	27.5	0.8	0.2		
275	1093	58	L.Sp.P.	L.	17.7	1.9	60.9	5.0	14.5	0.34	3.12
				Sp.	71.9	27.9	0.1	0.1	0.0		
				P.	77.1	8.5	14.2	0.1	0.1		
334	1143	696	L.Sp.P.	L.	20.9	2.3	58.2	4.9	13.7	0.36	3.13
				Sp.	74.0	25.7	0.2	0.1	0.0		
				P.	78.3	7.6	14.0	0.1	0.0		
				Equilibria [Liquid + Spinel + Melilite + Air]							
230	1093	51	L.Sp.Mel.	L.	9.5	4.8	67.2	4.6	13.9	0.33	3.63
				Sp.	67.4	32.3	0.3	0.0	0.0		
				Mel.	1.1	22.7	9.2	32.0	35.0		
312	1113	691	L.Sp.Mel.	L.	6.2	8.7	67.1	4.0	14.0	0.29	3.73
				Sp.	66.9	32.6	0.4	0.0	0.1		
				Mel.	0.5	22.2	10.3	30.8	36.2		
300	1113	61	L.Sp.Mel.	L.	8.9	8.8	64.9	3.8	13.6	0.28	3.73
				Sp.	67.0	32.2	0.4	0.0	0.4		
				Mel.	0.7	22.6	9.5	31.4	35.8		
299	1123	61	L.Sp.Mel.	L.	9.6	10.0	61.2	5.0	14.2	0.35	3.19
				Sp.	66.2	32.6	0.6	0.1	0.5		
				Mel.	0.7	22.5	8.6	32.0	36.2		
298	1123	62	L.Sp.Mel.	L.	7.8	13.1	61.7	4.1	13.3	0.31	3.55
				Sp.	66.7	32.8	0.4	0.1	0.0		
				Mel.	0.5	22.5	9.0	31.4	36.6		
297	1133	62	L.Sp.Mel.	L.	7.9	13.3	60.1	4.7	14.0	0.34	3.21
				Sp.	66.9	32.6	0.4	0.0	0.1		
				Mel.	0.6	22.7	7.9	32.1	36.7		
				Equilibria [Liquid + Spinel + Hematite + Air]							
269	1193	58	L.Sp.Hem.	L.	22.8	3.5	44.3	7.5	21.9	0.34	1.51
				Sp.	77.6	22.1	0.1	0.1	0.1		
				Hem.	99.9	0.0	0.1	0.0	0.0		
362	1243	697	L.Sp.Hem.	L.	26.6	3.2	43.1	7.1	20.0	0.36	1.59
				Sp.	82.6	17.2	0.1	0.1	0.0		
				Hem.	99.8	0.2	0.0	0.0	0.0		
362	1243	697	L.Sp.Hem.	L.	28.9	2.5	52.1	4.3	12.2	0.35	3.16
				Sp.	80.2	19.6	0.1	0.1	0.0		
				Hem.	99.8	0.2	0.0	0.0	0.0		
				Equilibria [Liquid + Hematite + Magneto-Plumbite + Air]							
262	1023	50	L.Hem.P.	L.	15.4	0.0	64.4	5.2	15.0	0.35	3.19
				Hem.	99.8	0.0	0.2	0.0	0.0		
				P.	79.3	0.1	19.9	0.2	0.5		
240	1043	50	L.Hem.P.	L.	15.3	0.0	64.6	5.2	14.9	0.35	3.21
				Hem.	99.9	0.0	0.1	0.0	0.0		
				P.	79.1	0.1	20.3	0.2	0.3		

Table II. Experimental Data on the Section $CaO/SiO_2 = 0.35$ and $PbO/(CaO + SiO_2) = 3.2$—Continued

Experiment Number	Temperature (°C)	Mixture Number	Phases in Equilibrium	Phase Name	Phase Composition (Wt Pct) Fe_2O_3	ZnO	PbO	CaO	SiO_2	C/S Wt	P/CS Wt
Equilibria [Liquid + Hematite + Magneto-Plumbite + Air]-Continued											
267	1063	50	L.Hem.P.	L.	16.6	0.0	63.1	5.2	15.1	0.34	3.11
				Hem.	99.9	0.0	0.0	0.0	0.1		
				P.	80.7	0.1	18.9	0.1	0.2		
276	1093	59	L.Hem.P.	L.	18.2	1.8	59.9	5.1	15.0	0.34	2.98
				Hem.	99.8	0.1	0.1	0.0	0.0		
				P.	78.7	1.0	20.1	0.1	0.1		
303	1123	59	L.Hem.P.	L.	20.6	1.7	59.4	4.7	13.6	0.35	3.25
				Hem.	99.8	0.1	0.1	0.0	0.0		
				P.	78.7	0.8	20.2	0.1	0.2		
335	1143	697	L.Hem.P.	L.	21.2	2.2	57.7	4.8	14.1	0.34	3.05
				Hem.	99.8	0.1	0.1	0.0	0.0		
				P.	78.7	6.9	14.2	0.1	0.1		
Equilibria [Liquid + Zincite + Melilite + Air]											
238	1143	55	L.Z.Mel.	L.	3.4	16.9	60.7	4.8	14.2	0.34	3.19
				Z.	0.1	99.9	0.0	0.0	0.0		
				Mel.	0.3	23.0	8.8	31.4	36.5		
237	1143	54	L.Z.Mel.	L.	0.0	17.0	64.0	4.6	14.4	0.32	3.37
				Z.	0.0	99.7	0.2	0.0	0.1		
				Mel.	0.0	23.4	8.2	31.8	36.6		
264	1153	54	L.Z.Mel.	L.	0.0	18.4	61.2	4.9	15.5	0.32	3.00
				Z.	0.0	99.9	0.0	0.1	0.0		
				Mel.	0.0	23.2	8.2	31.7	36.9		
Equilibria [Liquid + Willemite + Melilite + Air]											
258	1153	55	L.Z2S.Mel.	L.	6.3	27.9	36.0	7.6	22.2	0.34	1.21
				Z2S	0.2	72.7	0.0	0.1	27.0		
				Mel.	0.2	24.2	7.3	31.6	36.7		
Equilibria [Liquid + Spinel + Zincite + Melilite + Air]											
231	1093	52	L.Sp.Z.Mel.	L.	4.6	14.9	65.8	2.9	11.8	0.25	4.48
				Sp.	66.7	33.2	0.1	0.0	0.0		
				Z.	1.6	98.0	0.2	0.2	0.0		
				Mel.	0.7	23.6	9.5	31.5	34.7		
232	1093	53	L.Sp.Z.Mel.	L.	6.3	13.9	64.2	3.3	12.3	0.27	4.12
				Sp.	65.8	33.4	0.2	0.0	0.6		
				Z.	0.6	99.3	0.1	0.0	0.0		
				Mel.	0.6	23.4	8.8	32.0	35.2		
254	1123	53	L.Sp.Z.Mel.	L.	7.1	16.4	58.6	4.4	13.5	0.33	3.27
				Sp.	66.4	33.6	0.0	0.0	0.0		
				Z.	0.6	99.1	0.2	0.1	0.0		
				Mel.	0.4	23.4	7.2	32.0	37.0		
Equilibria [Liquid + Zincite + Melilite + Larsenite + Air]											
233	1093	54	L.Z.Mel.Lar.	L.	0.0	14.9	69.2	3.1	12.8	0.24	4.35
				Z.	0.0	99.3	0.5	0.1	0.1		
				Mel.	0.0	23.2	10.7	31.0	35.1		
				Lar.	0.0	24.1	54.8	3.6	17.5		
Equilibria [Liquid + Spinel + Hematite + Magneto-Plumbite + Air]											
333	1193	697	L.Sp.Hem.P	L.	25.6	2.1	54.9	4.4	13.0	0.34	3.16
				Sp.	78.0	21.6	0.3	0.1	0.0		
				Hem.	99.8	0.1	0.1	0.0	0.0		
				P.	79.5	6.7	13.7	0.1	0.0		
Equilibria [Liquid + Hematite + Magneto-Plumbite + Wollastonite + Air]											
255	993	50	L.Hem.P.CS	L.	11.7	0.0	70.4	3.7	14.2	0.26	3.93
				Hem.	99.7	0.0	0.1	0.1	0.1		
				P.	80.2	0.0	19.6	0.1	0.1		
				CS.	0.4	0.0	1.7	47.0	50.9		

Since the FeO concentrations in the present system in air are not high, then the liquidus surface approaches the composition plane of ZnO-($PbO + CaO + SiO_2$)-Fe_2O_3 (Figure 1). Therefore, the error involved in the projection of the "two-dimensional liquidus surface" with isotherms, "univariant lines," and "invariant points" onto the composi-

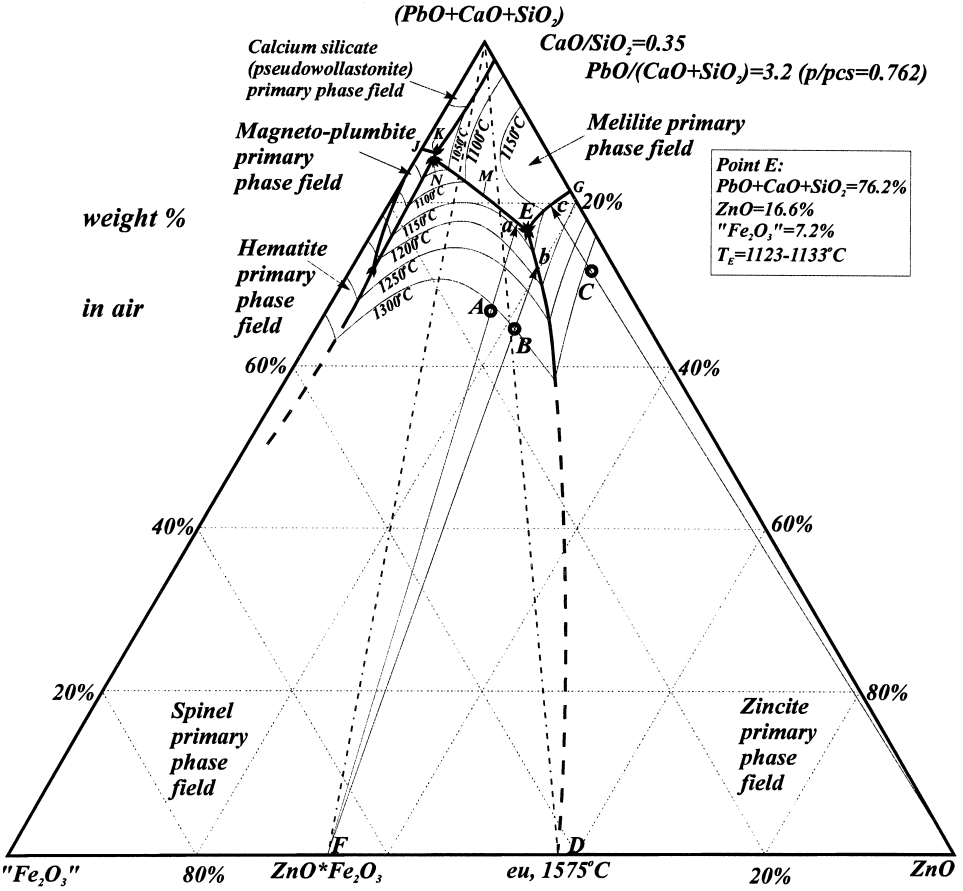

Fig. 2—Experimentally determined liquidus surface on the pseudoternary section ZnO-"Fe_2O_3"-(PbO + CaO + SiO_2) with weight ratios CaO/SiO_2 = 0.35 and $PbO/(CaO + SiO_2)$ = 3.2 in air.

tion plane ZnO-(PbO + CaO + SiO_2)-Fe_2O_3 is not significant (effectively, all iron is assumed to be present as Fe_2O_3).

C. *Quenching Technique with Electron Probe X-Ray Microanalysis*

The experimental technique used in the present study is essentially similar to that used in other studies by the authors.[9–22] In brief, artificial slag samples were equilibrated at high temperature in a controlled atmosphere (air, in the present case). The bulk composition and temperature for each experiment were deliberately selected so that at least one crystalline solid was present in equilibrium with the liquid. Samples were quenched, mounted in resin, and polished. The compositions of the glass (liquid) and crystalline solids were measured with the electron probe X-ray microanalysis (EPMA) technique. Discussions on features, advantages, and details of the experimental technique can be found in previous publications by the authors.[9–22] Details of the experimental technique that are particularly important to the present study are discussed subsequently.

Powders of PbO, SiO_2, ZnO, Fe_2O_3, and $CaSiO_3$ of 99.5 + wt pct purity were used as starting materials. The powders were calcined, mixed in the desired proportions, and melted in platinum crucibles to obtain intermediate master slags. If the mixtures are made directly from pure oxide powders, then PbO-rich liquid is formed during equilibration at high temperatures. The presence of high-melting-temperature oxides can make attainment of equilibrium difficult to achieve, forcing extension of the equilibration time. These lead to high PbO losses through vaporization before all components are dissolved. For these reasons, a series of glassy PbO-SiO_2 master slags was prepared, with fusion temperatures below 800 °C (1073 K), and these were then introduced into the mixture. Note that the PbO activity in the silicate melts exhibits a strong negative deviation that results in the relatively lower PbO equilibrium vapor pressures and, therefore, relatively lower PbO vaporization rates from the lead-silicate liquid.

The master slags were then ground in an agate mortar and mixed with appropriate additions of pure oxide powders, pelletized, and equilibrated in platinum crucibles covered with lids, usually in two steps. The first step was to premelt the sample at a temperature higher than the final equilibration temperature to ensure that the sample was homogeneous. The sample was then equilibrated at the desired lower final temperature for a time sufficient to achieve equilibrium. Equilibration times between 1 and 20 hours were used in the present study, depending on the mixture composition and temperature. In general, for lower temperatures or mixtures having higher silica contents, longer treatment times were employed. Particular attention was given to confirming the attainment of local equilibrium in each experiment. A number of indicators and approaches were applied for this purpose. First, experiments with different equilibration times

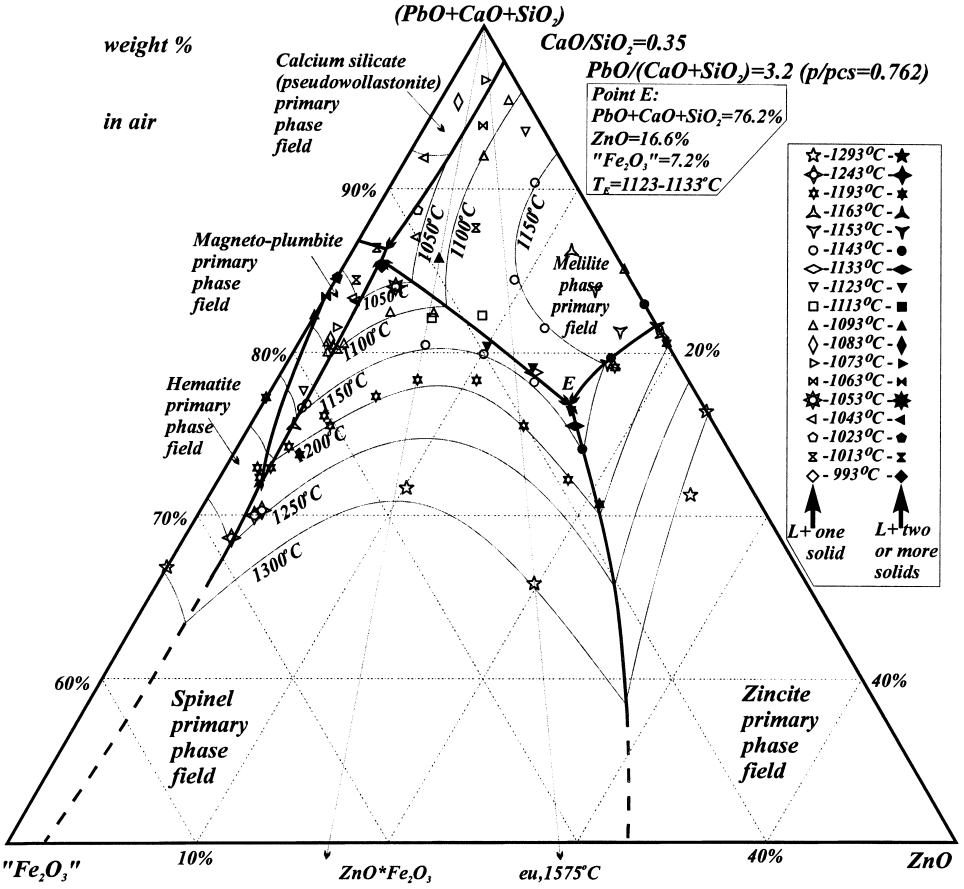

Fig. 3—Part of the experimentally determined liquidus surface on the pseudoternary section ZnO-"Fe_2O_3"-(PbO + CaO + SiO_2) with weight ratios CaO/SiO_2 = 0.35 and $PbO/(CaO + SiO_2)$ = 3.2 in air with experimental points.

were conducted for representative samples. The independence of the result on the equilibration time was taken as an indication of the attainment of equilibria. Much longer times were then selected for further experiments. Note that using the present technique, long equilibration times are possible without prejudicing the experimental outcome, since chemical analysis is undertaken after the experiment is completed and the accuracy of the final results is independent of bulk lead oxide content changes during equilibration. Second, the use of the electron probe makes it possible to directly measure the homogeneity of the glass-phase composition across the sample. A uniform composition is taken to mean that the equilibrium has been achieved. Note that each reported phase composition is an average of a minimum of five to ten measurements within that phase, performed in various parts of the sample. If the composition of the glass phase is shown to vary with location within the sample, this indicates incomplete equilibration. The experiment is then repeated until this effect is eliminated. Attention has also been given to the morphology, shape, and compositions of the solid crystallized phases: the presence of crystals homogeneous in composition, with well-developed facets, was taken as further indication of the attainment of equilibrium.

The experimental program at each step was based on the critical evaluation of data that had just been obtained. That is, successive experiments were chosen so as to predict more closely the liquidus surface in the remaining areas of uncertainty and to assist in the planning of further experiments. The information on melt behavior, such as rates of achievement of equilibrium, determined in closely related preceding areas in terms of temperature and composition, was used to choose appropriate procedures for each particular next experiment, including selection of temperatures and times for two-step equilibration.

The furnace temperature was controlled to within ±1 K. The Pt/Pt-13 pct Rh working thermocouple placed adjacent to the sample was periodically tested against a calibrated standard thermocouple. The overall temperature accuracy was estimated to be ±5 K. After equilibration, samples were quenched in iced water, dried, and weighed. Sample weights were monitored before and after the experiments. All weight measurements were performed on an analytical balance with an accuracy of ± 0.1 mg. Samples then were mounted and polished so that whole sections of the melt, from wall to wall and from top to bottom, could be examined. This enables any segregation of the phases during equilibration to be detected.

The microstructures were examined in detail using optical microscopy as well as scanning electron microscopy (SEM) coupled with an energy-dispersive spectra (EDS) analyzer. Phase composition analysis was then carried out with a JEOL* 8800L electron probe microanalyzer (EPMA) with wavelength-dispersive detectors. An accelerating voltage of

*JEOL is a trademark of Japan Electron Optics Ltd., Tokyo.

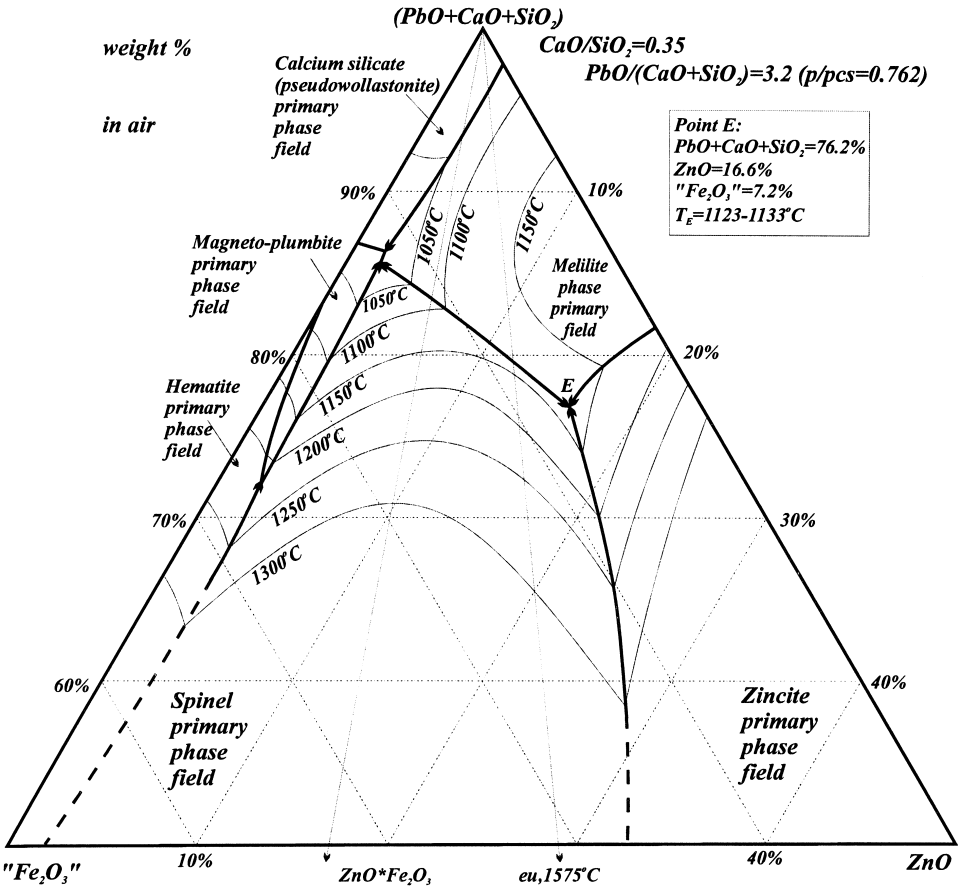

Fig. 4—Part of the experimentally determined liquidus surface on the pseudoternary section ZnO-"Fe_2O_3"-(PbO + CaO + SiO_2) with weight ratios CaO/SiO_2 = 0.35 and PbO/(CaO + SiO_2) = 3.2 in air.

15 kV and a probe current of 15 nA were used. A wollastonite ($CaSiO_3$) standard** was used for calcium and silicon, a willemite (Zn_2SiO_4) standard† was used for zinc, a hematite (Fe_2O_3) standard** was used for iron, and a lead-silicate glass standard‡ (Pb = 65.67 ± 0.26, Si = 13.37 ± 0.24, and O = 20.35 wt pct) was used for lead. The Duncumb–Philibert ZAF correction procedure supplied with the JEOL-8800L microanalyzer was applied. Careful selection of standards helped to ensure that the average accuracy of the EPMA measurements was within ±1 wt pct. The X-ray diffraction (XRD) analysis was used in some cases to confirm phase identification. The XRD analysis was carried out with a PHILIPS§ PW1130 X-ray diffractometor with a graphite monochromator, using Cu $K\alpha$ radiation.

**Charles M Taylor Co., Stanford, CA.

†Micro-Analysis Consultants Ltd, Cambridge, United Kingdom.

‡Office of Standard Reference Materials, National Institute of Standards and Technology, Gaithersburg, MD.

§PHILIPS is a trademark of Philips Electronic Instruments Corp., Mahwah, NJ.

The loss of PbO during equilibration is one major difficulty in the present experimental technique, since the pseudoternary sections are constructed for certain ratios of PbO/(CaO + SiO_2). Special measures were undertaken to reduce PbO losses during equilibration. Lead-silicate master slags were prepared first for this reason, to incorporate PbO into a silicate glass. Crucibles were covered with a platinum lid. The use of the lid, in conjunction with other measures, minimized PbO losses and, importantly, made these losses more predictable. Homogenization treatment of the sample at lower temperatures (of about 850 °C to 900 °C) was applied in some cases before a high-temperature premelt, to ensure that the high-PbO material was incorporated into the molten silicate before being exposed to higher temperatures. The PbO vaporization rates were monitored for a range of mixtures and equilibration temperatures. Excess PbO was added to the mixtures, so that following equilibration, the desired final melt composition was obtained. The accuracy of these corrections was checked by EPMA measurements of the liquid compositions after the experiments. The EPMA was used to control the homogeneity of the liquid phase, which meant that even though vaporization took place during the experiment, the equilibrium was achieved between the condensed phases. Similar to the selection of equilibration times (as discussed previously), successive planning of experiments was used to assist in the selection of procedure parameters for each individual experiment. The information on melt behavior in relation to the PbO losses, determined in closely related temperatures and compositions, was used to choose appropriate compositional adjustments for subsequent experiments. Although experiments were carefully planned to overcome this problem and to obtain a liquid composition with exactly or nearly the selected ratio with a minimum number of experiments, this, in general, could not be achieved by the first experiment. This meant that

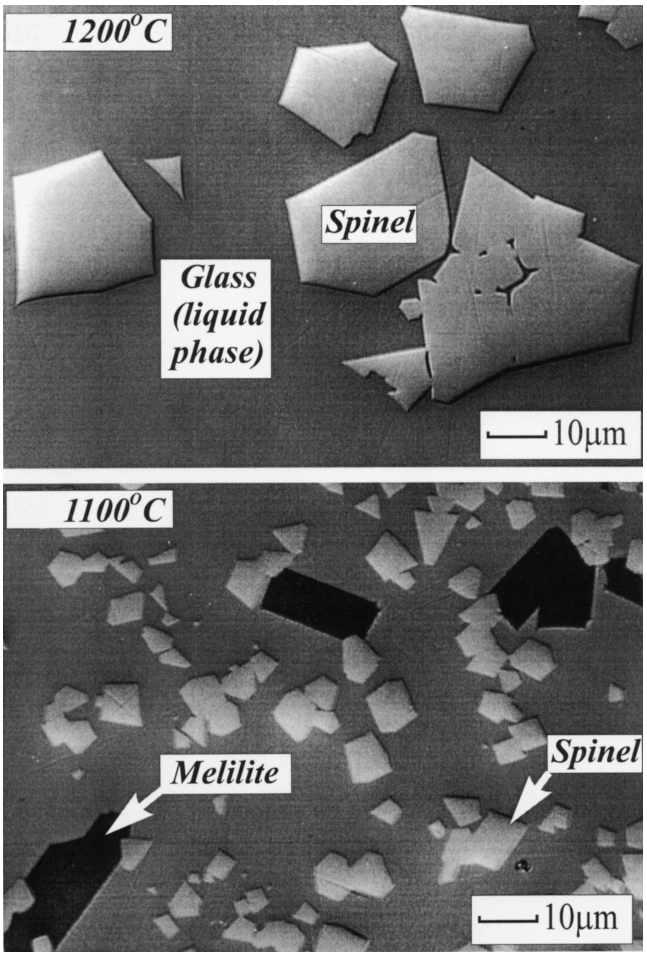

Fig. 5—Photomicrograph of mixture A quenched from (*a*) 1200 °C and (*b*) 1100 °C.

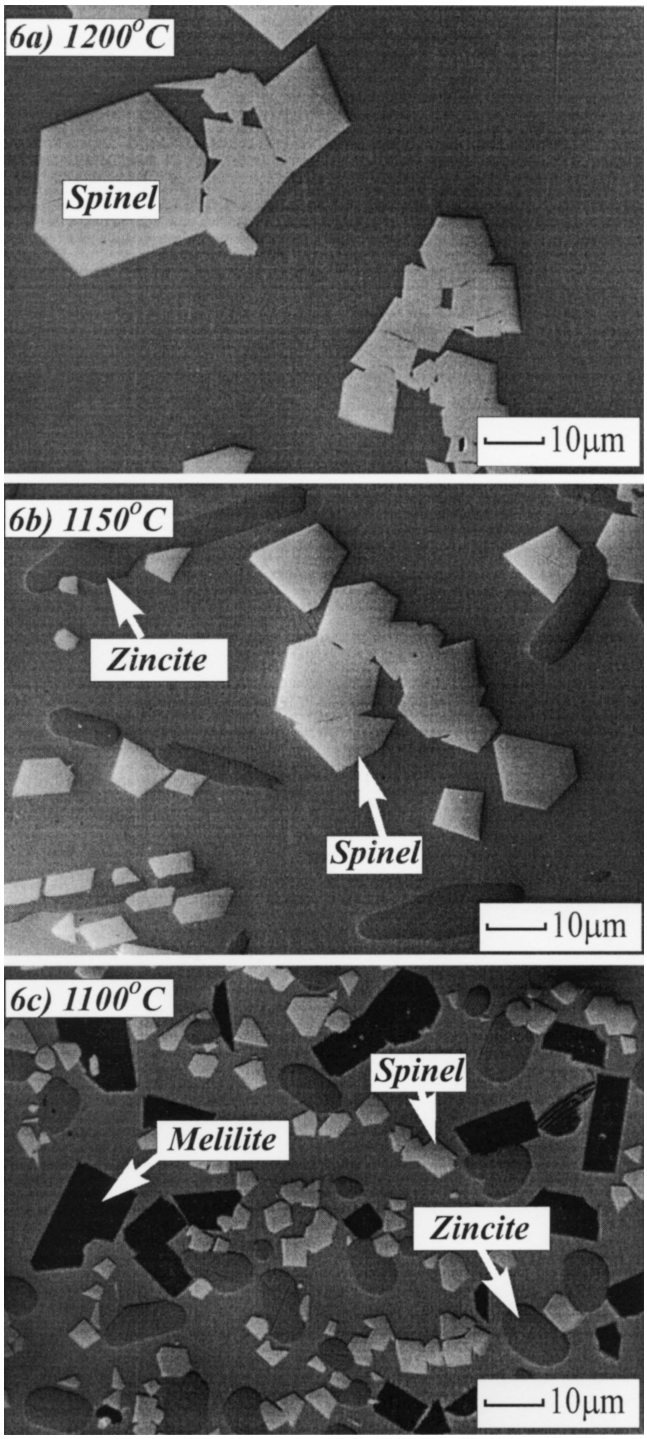

Fig. 6—Photomicrograph of mixture B quenched from (*a*) 1200 °C, (*b*) 1150 °C, and (*c*) 1100 °C.

it was necessary to repeat some experiments. Only those experiments with the liquid having $PbO/(CaO + SiO_2)$ and CaO/SiO_2 ratios near the selected ones were chosen for the construction of the pseudoternary section. Other data points are reported for subsequent use in thermodynamic modeling of the system.

Application of the EPMA to the examination of the samples brings a number of advantages to the phase-equilibrium study. One of the advantages of the present experimental technique, particularly important for lead- and zinc-containing systems at high temperatures, is the elimination of the inaccuracies associated with the bulk-sample composition changes through lead and zinc oxide vaporization at high temperatures. In the present case, changes in the bulk composition do not affect the final results, since the chemical compositions of all phases are measured after completion of the experiment. It is particularly this advantage of the experimental technique that enabled the study of PbO-containing slags exhibiting noticeable PbO losses due to vaporization to be successfully performed.

Another important advantage of the technique is that each experiment provides information on the liquidus composition and on the compositions of the solid phases formed. This greatly increases the productivity of the research and gives information on the extensive solid solutions found in these systems. The efficiency of the work is greater, since, for most of the cases, one mixture is used for several experiments, and usually each single experiment, which contains at least one solid in equilibrium with liquid, provides liquidus and solidus information. This experimental technique has enabled the comprehensive characterization of this complex multicomponent system relevant to the zinc and lead smelting production to be performed.

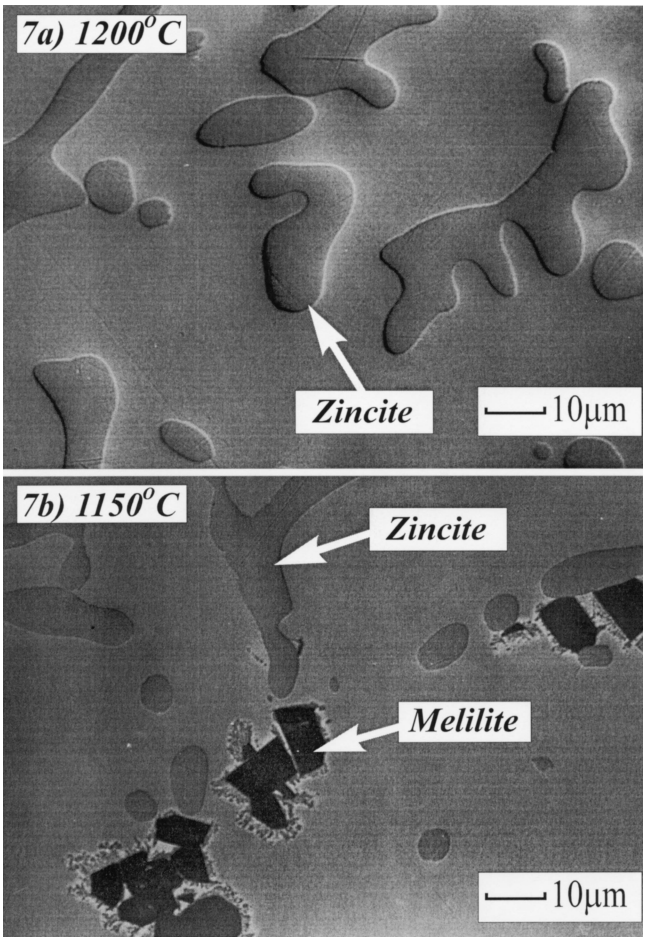

Fig. 7—Photomicrograph of mixture C quenched from (*a*) 1200 °C and (*b*) 1150 °C.

III. RESULTS

The artificial mixture compositions used for the equilibration experiments are given in Table I. The results of 138 quenching experiments are given in Table II. Each phase composition given in Table II is an average of up to ten compositions measured in various locations within that phase.

These data were used to construct the pseudoternary section of the multicomponent system PbO-ZnO-CaO-SiO_2-"Fe_2O_3" with a CaO/SiO_2 weight ratio of 0.35 and a PbO/(CaO + SiO_2) weight ratio of 3.2 (Figures 2 through 4). Note that only points with compositional ratios equal or close to the selected section were used to determine liquidus isotherms and boundary lines (refer to the experimental points plotted in Figure 3). In addition, general trends as a function of changes in the CaO/SiO_2 and PbO/(CaO + SiO_2) ratios were also taken into account. The pseudoternary section has primary fields of spinel (zinc ferrite, $Zn_xFe_{3-y}O_{4+z}$), zincite ($Zn_uFe_{1-u}O$), melilite ($Pb_vCa_{2-v}Zn_wFe_{1-w}Si_2O_7$), hematite ($Fe_2O_3$), magnetoplumbite ($PbFe_{10}O_{16}$), and wollastonite ($CaSiO_3$). Magnetite ($Fe_3O_4$) and franklinite ($ZnFe_2O_4$) are isomorphous (spinels) and form a continuous range of zinc ferrite solid solutions.[26] The present experiments in the low-zinc-oxide region indicate that the composition of spinel in equilibrium with the liquid phase approaches the franklinite composition ($ZnO \cdot Fe_2O_3$) in air in the range of temperatures investigated. Magnetoplumbite, on cooling, forms as a result of an incongruent reaction between liquid and either hematite or zinc ferrite. Magnetoplumbite can exist in equilibrium with calcium silicate (line KN).

Since the zincite and spinel phases do not contain significant amounts of PbO, CaO, or SiO_2 in solid solution, then EPMA measurements of the glass compositions were sufficient to construct "liquidus surfaces" in the primary-phase fields of zincite and spinel. Repeated quenching experiments from various temperatures, however, had to be performed in other primary-phase fields.

The spinel, zincite, and melilite primary-phase fields intersect at the boundary lines DE, GE, and NE; the junction of these lines is the special point E, with the minimum liquidus temperature. The boundary line NE has been found by experiment to have a temperature maximum at point M. The point N is at a lower temperature than point E. Point E has been approximately located at a (PbO + CaO + SiO_2) level of 76.2 wt pct, a ZnO level of 16.6 wt pct, an "Fe_2O_3" level of 7.2 wt pct, and a temperature (T_E) between 1123 °C and 1133 °C.

General ternary-phase diagram rules can be applied only in the primary fields of zincite, hematite, and spinel. As melilite, calcium silicate, or magnetoplumbite are formed as the temperature decreases, the liquid compositions leave the section because the compositions of these solids do not lie on the section. However the liquidus temperatures for compositions in the primary fields of melilite, calcium metasilicate, and magnetoplumbite can still be uniquely defined.

Examples of microstructures observed at different temperatures and compositions are presented in Figures 5 through 7. Composition A in Figure 2 approximately corresponds to the average Lead Isasmelt slag composition.[13] Spinel is the first phase to form on crystallization of sample A (Figure 5(a)). On cooling further, spinel precipitation takes place and the liquid composition moves in the direction Aa, which is an extension of the line FA. When the liquid composition reaches the boundary line at point a, melilite starts to precipitate (Figure 5(b)), and the liquid composition leaves the present section.

The crystallization of sample B is illustrated in Figure 6. Spinel is the first solid to form (Figure 6(a)). When the liquid composition reaches the boundary line of zincite-spinel (point b), coprecipitation of zincite and spinel begins (Figure 6(b)) and the liquid composition moves along the boundary line DE from point b to E. At the special point E, melilite starts to precipitate (Figure 6(c)), and the liquid composition leaves the composition section.

Figure 7 illustrates the microstructures formed on crystallization of sample C. The first solid to form is zincite (Figure 7(a)); on cooling, the liquid composition reaches the boundary line at point c, melilite starts to precipitate together with zincite (Figure 7(b)), and the liquid composition leaves the composition section.

The microstructures presented in Figures 5 through 7 illustrate the crystallization sequences that can take place in the real lead slags and demonstrate the morphologies of the crystalline phases obtained in the laboratory experiments.

IV. CONCLUSIONS

Preliminary studies of quenched industrial lead smelting slag and synthetic slags have allowed the selection of an

appropriate pseudoternary section through which to describe the multicomponent system PbO-ZnO-CaO-SiO_2-FeO-Fe_2O_3. The pseudoternary section ZnO-"Fe_2O_3"-(PbO + CaO + SiO_2) has been constructed with a CaO/SiO_2 ratio of 0.35 and a PbO/(CaO + SiO_2) ratio of 3.2 in a range of compositions close to the low-lead Isasmelt slag. This section describes the liquidus temperatures of the slags as a function of composition. The diagram enables the proportions of primary solid phases present to be predicted in selected primary-phase fields. The slag-chemistry plant data can be systematically recorded and analyzed, and further optimization of the fluxing practice can be conducted.

The pseudoternary sections can also be used to improve the understanding of the mechanisms of accretion formation and provide a method for further systematic research on these phenomena.

In conclusion, the construction of the pseudoternary sections has improved our understanding of processes occurring in the lead smelting reactors and has provided a useful tool for process analysis.

ACKNOWLEDGMENTS

The authors thank the Australian Research Council (ARC) for providing financial support to enable this work to be carried out. The authors would like to thank Roger Playor, formerly Mt. Isa Mines, for his advice, help and encouragement in undertaking this research.

REFERENCES

1. W.J. Errington, J.H. Fewings, V.P. Keran, and W.T. Denholm: *Extraction Metallurgy '85 Symp.*, Institute of Mining and Metallurgy, London, 1985, pp. 199-208.
2. S.P. Matthew, G.R. McKean, R.L. Player, and K.E. Ramus: *Proc. World Symp. on Metallurgy and Environmental Control, Lead-Zinc '90*, TMS, Warrendale, PA, 1990, pp. 889-901.
3. W.McA. Manson, and E.R. Segnit: *Proc. Aus IMM*, 1956, No. 180, pp. 119-47.
4. T. Kato, Y. Sugawara, and A. Yazawa: *Bulletin of the Research Institute of Mineral Dressing and Metallurgy*, Tohoku University, Tohoku, 1979, vol. 35 (1), pp. 81-92.
5. J.G. Lenz and I. Lee: *Proc. 2nd Int. Symp. on Metallurgical Slags and Fluxes*, TMS-AIME, Warrendale, PA, 1980, pp. 823-35.
6. F.T. Lee: Ph.D. Thesis, The University of Queensland, Queensland, 1991.
7. F.T. Lee, J.D. Nairn, and P.C. Hayes: *Proc. Int. Conf. on Extractive Metallurgy of Gold and Base Metals*, Aus IMM, Parkville, Victoria, Australia, 1992, pp. 459-64.
8. J.D. Nairn: Ph.D. Thesis, The University of Queensland, Queensland, 1993.
9. E. Jak, B. Zhao, and P.C. Hayes: *Metall. Mater. Trans. B*, 2002, vol. 33B, pp. 865-76.
10. E. Jak, B. Zhao, and P.C. Hayes: *Metall. Mater. Trans. B.*, 2000, vol. 31B, pp. 1195-1201.
11. E. Jak, B. Zhao, and P.C. Hayes: *Metall. Mater. Trans. B*, 2002, vol. 33B, pp. 877-90.
12. E. Jak, N. Liu, P. Wu, A. Pelton, H.G. Lee, and P.C. Hayes: *Proc. 6th Aus IMM Extractive Metallurgy Conf.*, Brisbane, Aus IMM, Parkville, Victoria, Australia, 1994, pp. 253-59.
13. E. Jak, N. Liu, H.G. Lee, and P.C. Hayes: *Proc. 6th Aus IMM Extractive Metallurgy Conf.*, Brisbane, Aus IMM, Parkville, Victoria, Australia, 1994, pp. 261-68.
14. E. Jak, N. Liu, H.G. Lee, and P.C. Hayes: *Proc. Lead & Zinc '95 Int. Symp.*, Sendai, Japan, Mining and Materials Processing Institute of Japan, Japan, 1995, pp. 747-51.
15. E. Jak, H.G. Lee, and P.C. Hayes: *Kor. IMM J.*, 1995, vol. 1, pp. 1-8.
16. E. Jak, B. Zhao, and P.C. Hayes: *Proc. 5th Int. Symp. on Metallurgical Slags and Fluxes*, ISS, AIME, Sydney, ISS, Warrendale, PA, 1997, pp. 719-26.
17. E. Jak, S.A. Degterov, B. Zhao, A.D. Pelton, and P.C. Hayes: *Proc. Zinc and Lead Processing Symp.*, Calgary, Canadian Institute of Mining, Metallurgy, and Petroleum, Montreal, PQ, Canada, 1998, pp. 313-33.
18. E. Jak, N. Liu, and P.C. Hayes: *Metall. Mater. Trans. B*, 1998, vol. 29B, pp. 541-53.
19. E. Jak, B. Zhao, N. Liu, and P.C. Hayes: *Metall. Mater. Trans. B*, 1999, vol. 30B, pp. 21-27.
20. E. Jak, S.A. Degterov, B. Zhao, A.D. Pelton, and P.C. Hayes: *Metall. Mater. Trans. B.*, 2000, vol. 31B, pp. 621-30.
21. E. Jak, S.A. Degterov, A.D. Pelton, and P.C. Hayes: *Metall. Mater. Trans. B*, 2001, vol. 32B, pp. 793-800.
22. E. Jak, S. Degterov, P.C. Hayes, and A.D. Pelton: *Proc. 5th Int. Symp. on Metallurgical Slags and Fluxes*, ISS, AIME, Sydney, ISS, Warrendale, PA, 1997, pp. 621-28.
23. E. Jak, S. Degterov, P. Wu, P.C. Hayes, and A.D. Pelton: *Metall. Mater. Trans. B.*, 1997, vol. 28B, pp. 1011-18.
24. E. Jak, S. Degterov, P.C. Hayes, and A.D. Pelton: *Can. Met. Q.*, 1998, vol. 37 (1), pp. 41-47.
25. M. Kudo, E. Jak, P.C. Hayes, K. Yamaguchi, and Y. Takeda: *Metall. Mater. Trans. B.*, 2000, vol. 31B, pp. 15-24.
26. E. Jak, B. Zhao, and P. Hayes: *MINPREX, Int. Congr. on Mineral Processing and Extractive Metallurgy*, Melbourne, Oct. 2000, The Australasian Institute of Mining and Metallurgy, Carlton, Victoria, Australia, 2000, pp. 479-84.
27. S.A. Degterov, E. Jak, P.C. Hayes, and A.D. Pelton: *Metall. Mater. Trans. B*, 2001, vol. 32B, pp. 643-57.
28. E. Jak and P. Hayes: *Can. Metall. Q.*, 2002, vol. 41 (2), pp. 163-74.